Measuring Dynamic Characteristics of the Human Arm in Three Dimensional Space

Mark C. Pierre and Robert F. Kirsch
Biomedical Eng. Dept., Case Western Reserve University, 10900 Euclid Ave, Cleveland, OH 44106
*E-mail:mcp6@po.cwru.edu

Abstract

The goal of this work was to develop a method to measure the dynamic characteristics of the human arm under natural three-dimensional conditions. Endpoint stiffness, which characterizes the relationship between hand displacements and the forces required to effect those displacements, was estimated during the application of three-dimensional, stochastic displacement perturbations to hand position. A nonparametric system identification algorithm was used to estimate endpoint stiffness from the measured force and displacement data. Endpoint inertia, viscosity and elasticity parameters were fit to the identified system. A graphical technique was introduced to help visualize these complex dynamic parameters. The results illustrate the importance of studying the endpoint dynamics in three dimensions.

Introduction

Endpoint dynamics depend on inherent musculo-skeletal properties, skeletal geometry and neuromuscular interactions. Many neurophysiological studies of posture and movement have focussed on constrained systems, such as single muscle, single joint or movements confined to a horizontal plain [1-3]. Although there are practical reasons for these simplifications, it is difficult to develop a fundamental understanding of natural control of posture and movement from these constrained studies. The central nervous system can not simply string together several simplified systems, but must deal with the interactions between different neural muscular and skeletal structures. In fact it may be impossible to extrapolate important three-dimensional features from these simplified models. All studies thus far have examined the arm constrained to a two dimensional plan. It is important to examine the arm in its natural state, in three-dimensional space.

Methods

The dynamic stiffness of the human arm is the relationship between a displacement imposed at the endpoint of the arm and the forces that affect that displacement. When measuring the dynamic stiffness of the human arm there are three directions in which the arm can be displaced (X, Y, Z), resulting in three forces. Therefore, the arm represents a multiple-input multiple-output (MIMO) system with displacement as the input and force as the output. A linear MIMO can be decomposed into single-input, single-output (SISO) subsystems. This allows each subsystem to be identified using a frequency domain non-parametric MIMO system identification technique [4,6]. This technique identifies a transfer function for each SISO, assuming linearity about the endpoint in the presence of small displacements. The MIMO system and its decomposition into multiple SISO subsystems is shown in Figure 1.

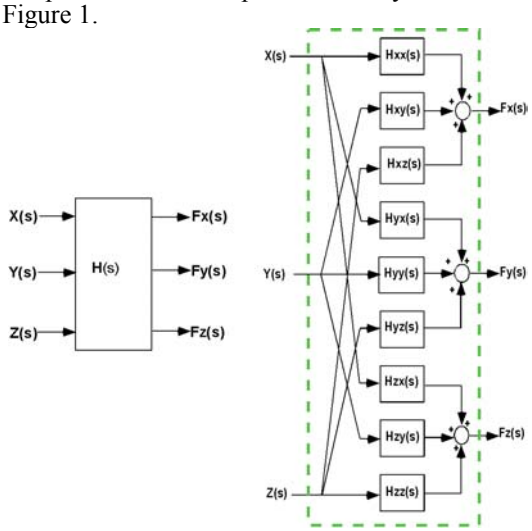

Figure 1. *SISO representation of endpoint stiffness dynamics*. Illustrates the decomposition of the endpoint stiffness dynamics into a group of SISO systems relating each endpoint displacement to each corresponding force.

The endpoint stiffness was estimated using data obtained during displacement perturbations applied to the hand of the human subject by a robotic manipulator [7]. The displacements and resulting forces were measured. Data from a single able-bodied subject is presented here. The subject was strapped into a rigid chair with custom supports to constrain both lateral and anterior-posterior trunk movements. The subject's arm was attached to the endpoint of a three-dimensional manipulator using a fitted fiberglass cast mounted inside a custom, heavy-duty gimbal. The gimbal allowed free rotation in all three directions about the endpoint of the hand. This removed any torques ensuring that the perturbation only applied translation.

An initially two-joint robotic manipulator [7] was adapted by adding a linear motor to its endpoint, allowing movement in all three axes. The manipulator was instrumented to measure endpoint force and position. These signals were anti-alias filtered at 200Hz, and sampled at 1kHz.

Measurements of endpoint stiffness were made with the endpoint of the arm level and approximately 0.3m anterior to the acromion. During each trial, the subject was instructed to exert a constant 30N force against the manipulator. The force was limited to 27 possible directions, corresponding to 3 axes (X, Y, Z) and 3 forces directions (pos., neg., none). The subject

was assisted in this task by a visual display of the endpoint force and the target force during each 30-second trial.

Figure 1 shows typical endpoint displacements and forces in the X direction for a single trial. During the perturbation, endpoint displacements had peak-to-peak amplitudes of approximately 3 cm. The resulting endpoint force amplitude varied from trial to trial depending on arm stiffness. The endpoint displacement frequency content was designed to be within the range of physiologically encountered perturbations [5] yet contain enough information for adequate identification of the endpoint dynamics. Figure 2 shows the spectra of the endpoint perturbations used in this experiment. These perturbations were flat to 3Hz, above which they decayed at a rate of roughly 20dB/decade.

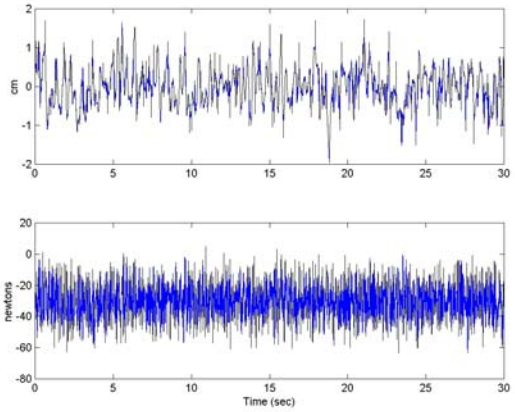

Figure 1. *Typical Data*. Endpoint displacements and forces measured in the X direction during a single trial.

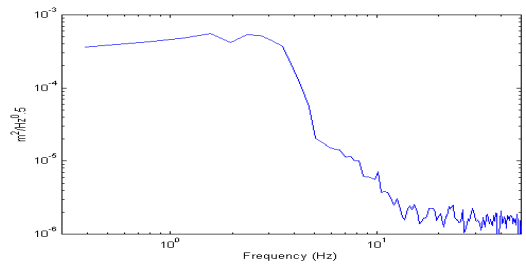

Figure 2. *Input displacement power spectrum*. Shows frequency range of the applied position perturbation.

This experimental technique has several benefits. First, using a stochastic input rather than a step reduces the possibilities of voluntary interactions because of the inputs random character. Also, the entire 3D-stiffness field can be swept during a relatively short experimental trial, rather then separate trials for each direction of interest. Finally, the dynamic input output identification can be obtained with little assumption about the systems structure.

It has been shown that inertial (I), viscous (B), and stiffness (K) parameters can represent SISO systems as shown in Equation 1.

$$\boldsymbol{H}_{ij}(\boldsymbol{s}) = \boldsymbol{I}_{ij}\boldsymbol{s}^2 + \boldsymbol{B}_{ij}\boldsymbol{s} + \boldsymbol{K}_{ij}, \text{ where } s = 2\pi f\sqrt{-1} \quad (1)$$

The parameterized system has the form specified by equation 2.

$$\left[\boldsymbol{I}_{end}\right]\begin{bmatrix}\ddot{x}\\ \ddot{y}\\ \ddot{z}\end{bmatrix} + \left[\boldsymbol{B}_{end}\right]\begin{bmatrix}\dot{x}\\ \dot{y}\\ \dot{z}\end{bmatrix} + \left[\boldsymbol{K}_{end}\right]\begin{bmatrix}x\\ y\\ z\end{bmatrix} = \begin{bmatrix}f_x\\ f_y\\ f_z\end{bmatrix}; \text{ where} \quad (2)$$

$$\left[\boldsymbol{I}_{end}\right] = \begin{bmatrix}\boldsymbol{I}_{xx} & \boldsymbol{I}_{xy} & \boldsymbol{I}_{xz}\\ \boldsymbol{I}_{yx} & \boldsymbol{I}_{yy} & \boldsymbol{I}_{yz}\\ \boldsymbol{I}_{zx} & \boldsymbol{I}_{zy} & \boldsymbol{I}_{zz}\end{bmatrix}, \left[\boldsymbol{B}_{end}\right] = \begin{bmatrix}\boldsymbol{B}_{xx} & \boldsymbol{B}_{xy} & \boldsymbol{B}_{xz}\\ \boldsymbol{B}_{yx} & \boldsymbol{B}_{yy} & \boldsymbol{B}_{yz}\\ \boldsymbol{B}_{zx} & \boldsymbol{B}_{zy} & \boldsymbol{B}_{zz}\end{bmatrix},$$

$$\left[\boldsymbol{K}_{end}\right] = \begin{bmatrix}\boldsymbol{K}_{xx} & \boldsymbol{K}_{xy} & \boldsymbol{K}_{xz}\\ \boldsymbol{K}_{yx} & \boldsymbol{K}_{yy} & \boldsymbol{K}_{yz}\\ \boldsymbol{K}_{zx} & \boldsymbol{K}_{zy} & \boldsymbol{K}_{zz}\end{bmatrix}$$

The inertial, viscous, and stiffness matrices were fit to the nonparametric transfer functions using a Nedler-Mead multi-dimensional optimization algorithm in Matlab.

The inertial, viscous, and stiffness properties are dependent on the direction of the input. Therefore these properties can be represented graphically as a function of direction. For stiffness, this is shown in Equation 3, where F represents the elastic components of the force in response to a unit three-dimensional displacement in endpoint position. An ellipsoid was created from this mathematical equation by plotting the force responses to the random unit displacement (F_x, F_y, and F_z) relative to one another. This is the extension of a previous two-dimensional method used to plot ellipses [1].

$$\begin{bmatrix}\boldsymbol{F}_x(\phi,\theta)\\ \boldsymbol{F}_y(\phi,\theta)\\ \boldsymbol{F}_z(\phi,\theta)\end{bmatrix} = \boldsymbol{K}_{end}\cdot\begin{bmatrix}\sin(\phi)\cdot\cos(\theta)\\ \sin(\phi)\cdot\sin(\theta)\\ \cos(\phi)\end{bmatrix}; \text{ where } \begin{matrix}0<\phi<2\pi\\ 0<\theta<2\pi\end{matrix} \quad (3)$$

Results

During one trial the subject exerted a 30N force simultaneously in the negative X direction and in the positive Z direction. The net force would be aimed in a region up and to the left of the subject's endpoint. The data analysis for this trial generated transfer functions for each SISO system. The parameters K, B, and I were fit to theses transfer functions. Figure 3 shows the actual transfer functions measured using nonparametric MIMO system identification and the parametric approximations of these systems.

The stiffness matrix from the parametric fit is shown in Equation (3).

$$\boldsymbol{K} = \begin{bmatrix}-486 & 435 & 178\\ 852 & -1300 & 385\\ 188 & 84 & -485\end{bmatrix}\frac{\boldsymbol{newtons}}{\boldsymbol{meter}} \quad (3)$$

This stiffness matrix can be represented graphically as an ellipsoidal plot in three dimensions. Figure 4 shows

the ellipsoid as the central figure surrounded by three two-dimensional projections which aid in abstracting the three dimensional content of the ellipsoid. This figure is shaded to highlight the varying stiffness. Areas with the highest stiffness are shaded lightly and areas of low stiffness are dark. Notice that the three dimensional imaging incorporates lighting effects to accentuate the three-dimensional curvature of the ellipsoid and should not be confused with the stiffness shading. The ellipsoid shows that there is a significant component in the third dimension.

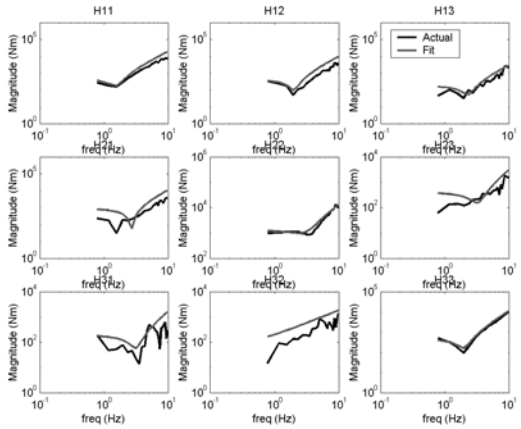

Figure 3. *Transfer functions*. Transfer functions measured from one trial and parametric fits. During this trial the subject exerted a (30N, 0, 30N) force.

Relative to the ellipsoidal plot, the subject would be oriented with their shoulders parallel to the X-axis facing the positive Y-direction. The arm would be level with the X-Y plane at a zero height along the Z-axis. The endpoint of the hand would be located in the center of the ellipsoid at location (0, 0,0).

Conclusions

This paper outlines a non-parametric method for characterizing thee-dimensional arm dynamics in response to stochastic perturbations. The method assumes no prior knowledge about the system dynamics except linearity in the presents of small displacements. In addition, this technique differs from previous techniques because it includes all three dimensions, allowing measurements of all neuromuscular interactions. Therefore, this test can be used to determine system structure completely and under natural three-dimensional conditions.
Preliminary results show that this method is suitable for characterizing changes in three-dimensional endpoint stiffness. In addition, the graphical ellipsoid is an important tool to help visualize the complex dynamic properties of the arm. Future work will concentrate on testing the dynamic properties of the arm in functional positions. Ultimately, this technique will be used to quantify the effects of FNS on the arm.

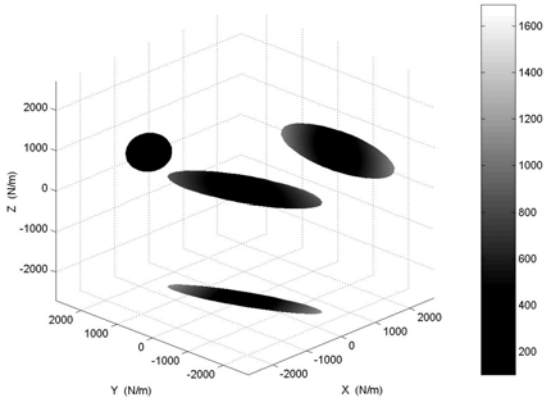

Figure 4. Three-Dimensional Stiffness Ellipsoid. The three-dimensional stiffness ellipsoid is the center most object. The three surrounding ellipses are projections of the ellipsoid onto each plane. Shading correlates to the magnitude of the stiffness, lighter being stiffer.

Acknowledgments

This work was supported by NIH HD32653 (RFK) and by training support to MCP (NIH 2T32GM07535-24 and NSF 9972747. Additional supported provided by the Cleveland VA FES Center.

References

[1] F. Mussa-Ivaldi, Hogan, N, Bizzi, E, "Neural, mechanical, and geometric factors subserving arm posture in humans." *The Journal of Neuroscience*, vol. 5, pp.2732-2743, 1985.
[2] J. M. Dolan, M. B. Friedman, and M. L. Nagurka, "Dynamic and loaded impedance components in the maintenance of human arm posture." *IEEE Transactions on Systems, Man, and Cybernetics*, vol. 23, pp. 698-709, 1993.
[3] T. Tsuji, Morasso, PG, Goto, K, Ito, K, "Hand impedance characteristics during maintained poster." *Biological Cybernetics*, vol. 72, pp. 475-485, 1995.
[4] J. S. Bendat and A. G. Piersol, Random Data: Analysis and Measurement Procedures. New York: Wiley, 1986
[5] Mann KA, Werner FW, Palmer AK, "Frequency spectrum analysis of wrist motion for activities of daily living." *The Journal of Orthopedic Research*, vol 7, pp. 304-306.
[6] E. J. Perreault, R. F. Kirsch, and A. M. Acosta, "Multiple-input, multiple-output system identification for the characterization of limb stiffness dynamics," Biol Cybern, vol. 80, pp. 327-337, 1999.
[7] A. M. Acosta, R. F. Kirsch, and E. J. Perreault, "A robotic manipulator for the characterization of two-dimensional dynamic stiffness using stochastic displacement perturbations," Journal of Neuroscience Methods, *102:177-86, 2000*.